# Patient-Specific Mappings between Myocardial and Coronary Anatomy

**Maurice Termeer[1], Javier Oliván Bescós[2], Marcel Breeuwer[2], Anna Vilanova[3], Frans Gerritsen[2], M. Eduard Gröller[4], and Eike Nagel[5]**

1 **Vienna University of Technology**
`maurice@cg.tuwien.ac.at`
2 **Philips Healthcare**
{`javier.olivan.bescos,marcel.breeuwer,frans.gerritsen`}`@philips.com`
3 **Eindhoven University of Technology**
`a.vilanova@tue.nl`
4 **Vienna University of Technology**
`groeller@cg.tuwien.ac.at`
5 **King's College London**
`eike.nagel@kcl.ac.uk`

**Abstract**

The segmentation of the myocardium based on the 17-segment model as recommended by the American Heart Association is widely used in medical practice. The patient-specific coronary anatomy does not play a role in this model. Due to large variations in coronary anatomy among patients, this can result in an inaccurate mapping between myocardial segments and coronary arteries. We present two approaches to include the patient-specific coronary anatomy in this mapping. The first approach adapts the 17-segment model to fit the patient. The second approach generates a less constrained mapping that does not necessarily conform to this model. Both approaches are based on a Voronoi diagram computation of the primary coronary arteries using geodesic distances along the epicardium in three-dimensional space. We demonstrate both our approaches with several patients and show how our first approach can also be used to fit volume data to the 17-segment model. Our technique gives detailed insight into the coronary anatomy in a single diagram. Based on the feedback provided by clinical experts we conclude that it has the potential to provide a more accurate relation between deficiencies in the myocardium and the supplying coronary arteries.

**1998 ACM Subject Classification** I.3.8 Applications, J.3 Life and Medical Sciences

**Keywords and phrases** Voronoi Diagram, Segmentation, Myocardium

**Digital Object Identifier** 10.4230/DFU.SciViz.2010.196

## 1 Introduction

In the field of cardiac tomography, the American Heart Association (AHA) has published a set of recommendations to standardize part of the clinical routine [4]. These recommendations concern the segmentation of the left ventricular myocardium, the heart muscle of the left ventricle. They also include a standardized nomenclature for the coronary arteries, small arteries surrounding the left ventricle that supply the myocardium with oxygenated blood. One of these recommendations is the use of a 17-segment model for the segmentation of the myocardium. This model defines a mapping of each of the segments to the coronary arteries that supply that region. The relation between the myocardium and its supplying coronary arteries is important during diagnosis.

The individual paths of the coronary arteries and the way they supply the myocardium varies greatly among different patients. This causes the standardized mapping between myocardial segments

Scientific Visualization: Advanced Concepts.
Editor: Hans Hagen; pp. 196–209

Dagstuhl Publishing
Schloss Dagstuhl – Leibniz Center for Informatics (Germany)

and coronary arteries to be of varying accuracy across different patients. This issue is acknowledged by the American Heart Association, with the note that the suggested model is based upon the methods available at that time [4].

With current MRI (Magnetic Resonance Imaging) technology it is possible to segment the three major coronary arteries from a whole heart scan [11]. The three primary coronary arteries are the left anterior descending (LAD), the left circumflex (LCX) and the right coronary artery (RCA). While there are still cases where a complete segmentation is not feasible, these issues will most likely be resolved in the near future.

We use the patient-specific coronary anatomy to improve the relation between the myocardium and the supplying coronary arteries. We explore two possible approaches. In our first approach we adapt the 17-segment model as defined by the AHA to fit to the coronary anatomy of the patient in question. In other words, we set a number of constraints to force the mapping between the myocardium and the areas the coronary arteries are supplying to correspond to the 17-segment model. In our second approach we do not set any constraints and thus allow for arbitrary mappings between the coronary arteries and the myocardium. Both approaches are based on Voronoi diagrams of the coronary arteries using geodesic distances along the epicardium, the outer part of the myocardium. The resulting relation divides the myocardium into several coronary territories, regions of the myocardium supplied by the coronary artery that corresponds to that territory. These territories, along with the coronary arteries themselves, are finally projected onto a two-dimensional bull's eye plot.

Both of our approaches result in customized diagrams that better reflect the actual relation between myocardial tissue and supplying coronary arteries. The approach of adapting the 17-segment model is less sensitive to incomplete segmentations of the coronary anatomy. On the other hand, unconstrained coronary territories may be more accurate for patients that do not correspond well to the 17-segment model.

Our article is structured as follows. We first give an overview of related work on the 17-segment model from the American Heart Association and patient-specific coronary territories in Section 2. In Section 3 we discuss the computation of the coronary territories and the projection on a bull's eye plot. In Section 4 we discuss both approaches to computing patient-specific coronary territories. In Section 5 we describe the results of an evaluation experiment and provide a use case of our techniques with viability data. In Section 6 we discuss the medical applications and issues of our approach. Finally, in Section 7 we conclude our work.

## 2 Related Work

The American Heart Association (AHA) published a set of recommendations to standardize the segmentation of the left ventricular myocardium [4]. This includes a division of the myocardium into 17 parts accompanied by a mapping of each of the segments to coronary territories. As a reference this 17-segment model is depicted in Figure 1. It shows the myocardium in a bull's eye plot, a two-dimensional representation of the left ventricle. Since its introduction, the 17-segment model has become widely accepted in clinical practice and it has replaced previous models. In the area of SPECT, for example, a 20-segment model [1] was more common prior to the introduction of the 17-segment model.

A medical study performed by Pereztol-Valdés *et al.* [10] using myocardial perfusion nuclear imaging gives a more precise relation between each of the 17 segments and the supplying coronary arteries. It shows that contrary to the model of the AHA, only nine segments are commonly supplied by one coronary artery; the remaining segments are supplied by multiple coronary arteries. It also verifies that there is great variability among patients, especially in the apical area of the left ventricle. Based on the outcome of this study, the authors presented a revised mapping of segments to coronary

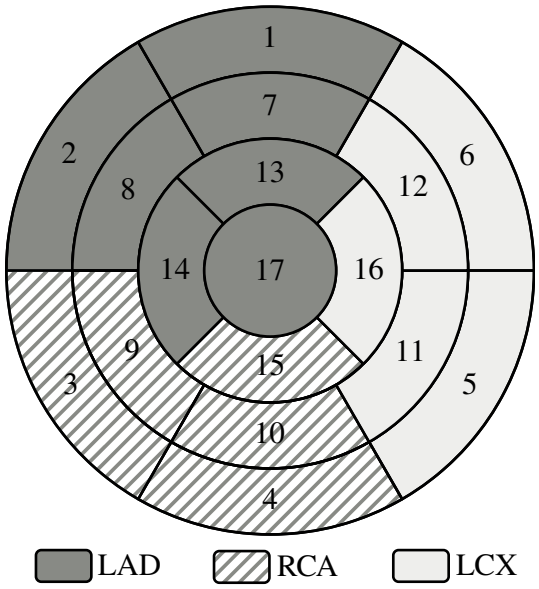


**Figure 1** The 17-segment model for the segmentation of the left ventricle as presented by the American Heart Association [4]. The patterns indicate the mapping of the segments to coronary territories.

territories, where some segments are assigned to multiple territories. Recently a similar study was published by Ortiz-Pérez *et al.* [9] using contrast-enhanced MRI. Their work also confirmed the variability in coronary anatomy and the need for a better model to more accurately attribute perfusion defects in segments to coronary arteries.

Beliveau *et al.* [2, 3] previously presented the idea of computing patient-specific coronary territories. In their work coronary arteries are segmented from a whole heart CT scan and projected on the segmented epicardial surface. The patient-specific coronary territories are computed by using a Voronoi diagram of the projected arteries. While their work is in several ways similar to ours, there are several key differences. Besides a different implementation approach and a different method to project the territories on a bull's eye plot, no explicit relation between the 17-segment model and the coronary territories is made, although the 17-segment model is mentioned in their work. Their approach is thus not capable of forcing correspondence to this model. We demonstrate how we can use this to regularize a bull's eye plot of viability data (see Section 5.2), while their approach is limited to showing an overlay. In other work, Voronoi diagrams are also being used for the analysis of modeled and segmented artery trees [6].

Oeltze *et al.* presented several novel visualization techniques for the analysis of perfusion data [8]. Their redefined bull's eye plot shows myocardial perfusion data of both rest and stress states in a single bull's eye plot based on the 17-segment model. They also presented an interactive bull's eye plot that is linked to a three-dimensional visualization showing coronary artery branches. Picking a segment on the bull's eye plot automatically adjusts the view of the three-dimensional view to show the corresponding artery.

## 3 Computation of Coronary Territories

A coronary territory defines the region of the myocardium supplied by a specific coronary artery. Determining which part of the myocardium a coronary artery is supplying is a complex and yet unsolved problem. We approach this by assuming that each part of the myocardium is supplied

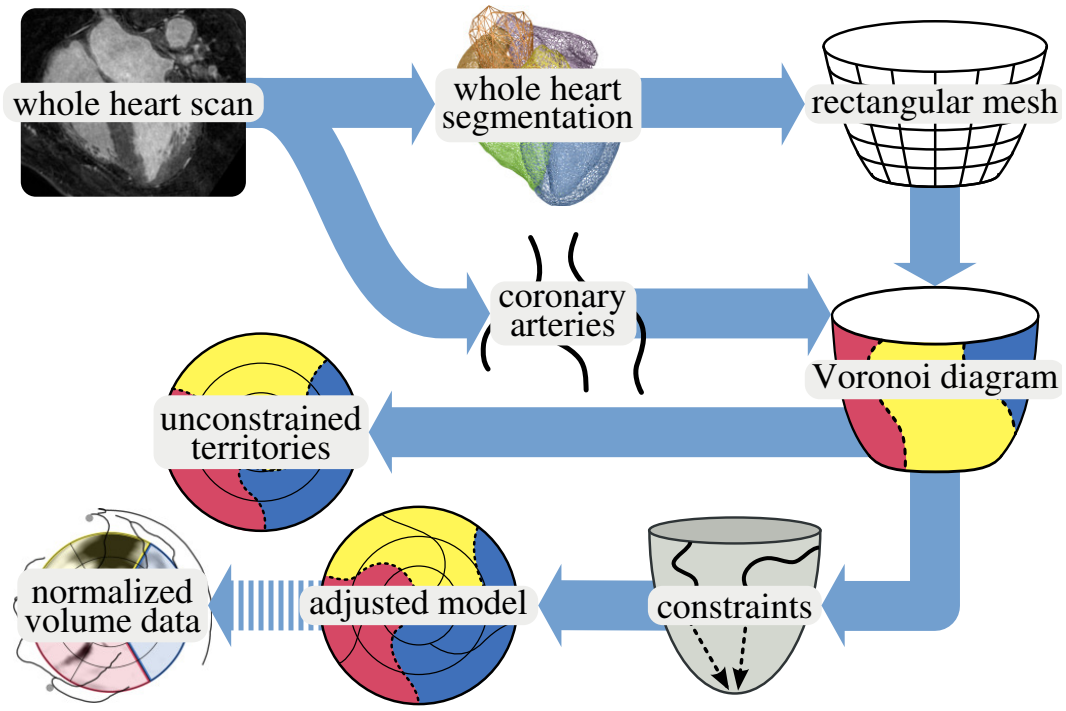


**Figure 2** Overview of our approach towards patient-specific coronary territories.

by its closest coronary artery. This approximation suffices for our purposes. We also perform all computations on the epicardial surface, instead of taking the three-dimensional nature of the myocardium into account.

An overview of our approach is shown in Figure 2. We obtain a whole heart segmentation from a whole heart MRI scan using an approach by Ecabert *et al.* [5]. Using only the left ventricular epicardium part of this segmentation, we create a rectangular mesh of the epicardium to gain more control over the resolution and uniformity of the mesh. We track the centerlines of the three primary coronary arteries in the same whole heart scan using a semi-automatic vessel tracking method [7] and project them onto the mesh of the epicardium. We subsequently compute a Voronoi diagram of these projected arteries. This diagram is finally projected on a bull's eye plot.

Prior to computing the Voronoi diagram, we can set a number of constraints to force the resulting division of the epicardium into coronary territories to correspond to the 17-segment model. In this case we can use the borders and middle lines of the coronary territories to adapt the 17-segment model to the patient. We can then also use the deviation between the original and adapted models to deform data from a different scan of the same patient to fit to the original 17-segment model. Without setting any constraints, the resulting coronary territories can have arbitrary shapes and need not correspond to the 17-segment model. Both these approaches are discussed in more detail in Section 4.

### 3.1 Mesh of the Epicardium

Our automatic segmentation algorithm gives a segmentation of the left ventricular epicardium in the form of an unstructured polygonal mesh. In order to guarantee a sufficient accuracy throughout the mesh during the Voronoi diagram computation we generate a rectangular mesh instead. We intersect the unstructured mesh with two sets of planes. One set consists of evenly spaced planes orthogonal to the long axis, the other set consists of planes through the long axis with evenly spaced angular

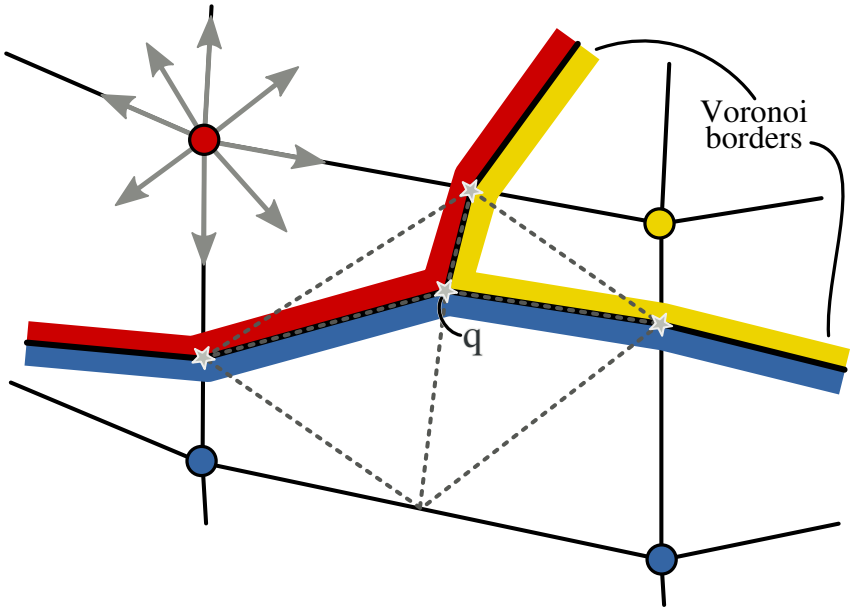


**Figure 3** The distances to the closest coronary artery are propagated to all neighbors of a vertex along the edges and diagonals of each quadrilateral it is part of. Each quadrilateral can be divided in up to four territories. The gray lines indicate the triangularization of this particular case. Note that our approach, opposed to the traditional marching squares algorithm, generates a vertex in the middle of the quadrilateral.

offsets to the short axis. The points at the intersections of a plane from each set and the unstructured mesh form control points for a set of interpolating Catmull-Rom spline patches. We generate the final rectangular mesh by tessellating each patch at the desired accuracy.

### 3.2 Projection of the Coronary Arteries

Once we have a proper mesh of the epicardium, we project the coronary arteries onto this mesh. We compute a discrete representation of the coronary artery tree by generating a set of points spaced approximately one millimeter apart along each coronary artery. For each of the points along each coronary artery, we compute the closest vertex of the mesh. The index of the artery and the Euclidean distance to that artery is stored at that vertex.

### 3.3 Computation of the Voronoi Diagram

As a first step towards computing the Voronoi diagram of the arteries on the epicardial mesh, we compute the closest coronary artery and the distance to that artery for all vertices of the mesh by propagating the information in the vertices encountered during the projection of the arteries in the previous step. Starting with an active set consisting of only those vertices, we propagate the distances to all neighboring vertices using an 8-neighborhood approach. In other words, each vertex has eight neighbors to which distances are propagated, except at the edges of the mesh (see Figure 3). Distances and indices to arteries are only updated if the distance is shorter than the one already present in the vertex, if any. Once the algorithm terminates, each vertex contains an index of and distance to its closest coronary artery.

Here “closest” refers to the distance along the epicardium to a projection of a coronary artery. We believe this method, although still very simple, approaches reality better than using Euclidean distances in space. Since we use a discrete mesh of the epicardium, the distance is the approximate

geodesic distance along this mesh. In order to obtain a good approximation of the true geodesic distance, we construct a sufficiently fine-grained mesh. In our experiments we construct a mesh with 80 contours between the apex and the base of the left ventricle and contours divided into 128 vertices. Experiments with using finer grained meshes indicate that the maximum error due to interpolation between vertices is less than one millimeter.

The Voronoi diagram is given by the lines passing through edges whose vertices have different closest coronary arteries. We extract these lines using an approach based on marching squares, as all faces of our mesh are quadrilaterals. The difference with traditional marching squares is that each quadrilateral can be divided in up to four parts. Figure 3 shows a case where the four vertices of a quadrilateral belong to three different coronary territories, dividing the quadrilateral into three parts. We have generalized the division of the quadrilateral to cover the cases where it needs to be divided into three or four parts. The intersection points on the edges of the quadrilateral are first computed. To improve the quality of the dividing lines, we use linear interpolation to compute more exact intersection positions. We then compute the average of these points, giving a point $q$ inside the quadrilateral. For edges that have no intersection point, we compute the point on the middle of those edges. We can then divide the quadrilateral into four regions where each region is given by one corner point, the two intersection or middle points of the edges connected to the corner and point $q$. Note that each of these four regions is always convex, as point $q$ is inside or on the rhombus spanned by the four intersection or middle points. The four regions can then be triangulated independently using at most two triangles, as is shown in Figure 3 by the gray dashed lines. The number of triangles used for parts consisting of multiple regions can be reduced. The blue part in Figure 3, consisting of two regions of the quadrilateral, can for example also be triangulated using three triangles. The edges of the Voronoi diagram are given by the edges of the triangles that belong to different parts.

### 3.4 Projection onto a Bull's Eye Plot

Once we have computed a complete Voronoi diagram on the epicardial surface, we project it onto a two-dimensional bull's eye plot. The projection method is based on a parameterization of the left ventricle, which is illustrated in Figure 4. Each point in the left ventricular myocardium can be specified using a 3-tuple $(\phi, h, r)$. In this tuple $\phi$ represents the angle with the short axis in a plane orthogonal to the long axis, $h$ the distance to the apex along the long axis and $r$ the distance to the long axis. The projection of the Voronoi edges is constructed by computing the parameters of all vertices and directly interpreting $(\phi, h)$ as polar coordinates. The coronary arteries are projected on the bull's eye plot using the same approach.

## 4 Patient-Specific Coronary Territories

In the 17-segment model there is no variation in shape among patients of the three coronary territories. Although this eases interpretation and comparison, it does not give any details about the patient-specific coronary anatomy.

Using the method of computing patient-specific coronary territories described above, we can improve on the 17-segment model in two different ways. The first approach is to alter the 17-segment model by fitting the model's edges to the patient-specific coronary territories. The second approach is to compute the coronary territories without taking any model into account.

### 4.1 A Patient-Specific 17-Segment Model

For the first approach to work, the morphology of the patient-specific coronary territories should match that of the 17-segment model. The first 16 segments of the 17-segment model divide the

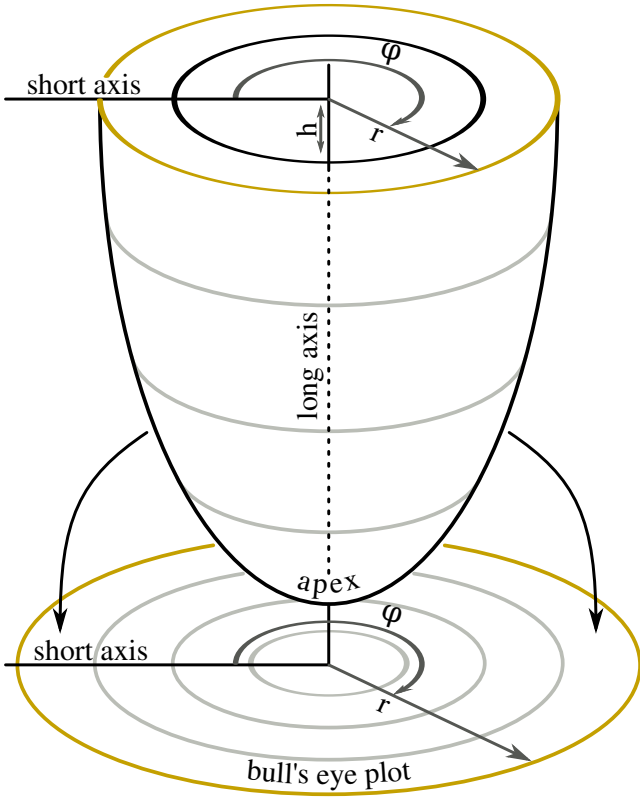


**Figure 4** Parameterization of the left ventricle and its mapping to a bull's eye plot.

left ventricle into three parts: a basal part, a mid-cavity part and an apical part. Each of these parts correspond to one of the rings in the model shown in Figure 1. Each of the primary coronary arteries supplies part of each of those three parts.

The segmentation of the coronary arteries in a whole heart MRI scan is a difficult task. As the coronary arteries become thinner towards the end, segmentation of the complete branch is rarely possible due to the resolution of current whole heart MRI scans. This often results in incomplete segmentations of the coronary arteries, which in turn causes the morphology of the coronary territories based on these segmentations to rarely match that of the 17-segment model. We can force a correspondence by artificially completing the segmentation of the coronary arteries by connecting the endpoint of each artery to the apex. This approach is a compromise between a solely segmentation-driven approach, like the approach discussed in Section 4.2, and a solely model-driven approach, like the 17-segment model.

When adapting the 17-segment model, the borders of the coronary territories in the model are fit to the corresponding borders in the Voronoi diagram. The edges of segments indicating the center of each territory are mapped to lines equidistant to the borders of that coronary territory. Both these mappings require that each coronary territory has two borders, i.e. it has a "left" and a "right" side. This means that each coronary territory should run from the apex to the base and should be connected, just as is the case in the 17-segment model.

The basal, mid-cavity and apical segments of the 17-segment model are equal thirds of the heart along the long axis. This means that any differences between the original and an adapted 17-segment model are strictly *angular* differences. The relation of the distance to the apex along the long axis is also preserved in the 17-segment model; adapting the model thus does not affect $h$. We conclude

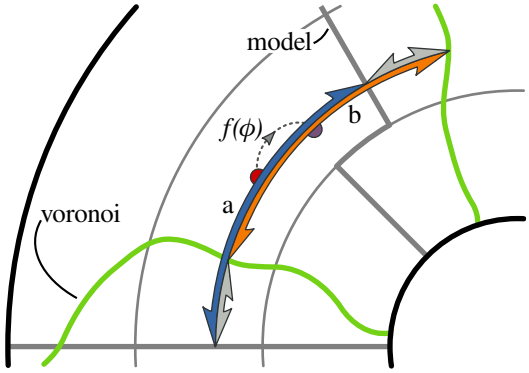


**Figure 5** Function $f$ transforms the query point (red dot) from the 17-segment model to the adapted model. The angular differences (gray arcs) are used to transform the blue arc A into the orange arc B.

that a function $f$ exists such that for any point $(\phi, h)$ in a bull's eye plot of the 17-segment model, $(f(\phi), h)$ gives the corresponding point in a bull's eye plot of an adapted 17-segment model.

Figure 5 gives an overview of the implementation of function $f$. Given a tuple $(\phi, r)$ in a coronary territory (the red dot), we compute the two angular differences between the borders of the coronary territory according to the 17-segment model and the Voronoi diagram respectively (the gray arcs), at distance $r$ from the apex along the long axis. We use linear interpolation between these two angular differences to find the angular difference for the specified value of $\phi$ (the arc marked $f$). This approach essentially transforms the blue arc A into the orange arc B using an angular scaling and translation. Note that function $f$ is in fact defined for every point inside the myocardium, even through it is only applied to the edges of the segments for computing the adapted 17-segment model. In Section 5.2 we use this property to adapt volume data to the 17-segment model instead, using the inverse of $f$.

Figure 6 shows a comparison between a standard 17-segment model (Figure 6a) and the same model adapted to the patient-specific coronary anatomy (Figure 6b). The coronary arteries are also projected on top of the bull's eye plots. Note that the Voronoi diagram is computed using geodesic distances in three-dimensional space, so the borders of the coronary territories generally are not equidistant to the coronary arteries between them. Also, part of the RCA wraps around the right ventricle. Since the distance to the long axis is lost in the bull's eye plot, this is no longer visible in the projection of the RCA. For this particular patient, the divergence from the model is not particularly big. This is not too uncommon, as the 17-segment model is based on an average of the population.

## 4.2 Unconstrained Coronary Territories

The previously discussed approach artificially completes the segmentation of the coronary arteries by connecting the end points to the apex. We can also omit this process and use the coronary anatomy directly. However, the resulting division of the myocardium into coronary territories does not necessarily correspond to the 17-segment model. Our experiments show that there is no complete correspondence for most patients. In most of the cases this is due to varying way the apex is supplied, as is confirmed by earlier studies [9,10]. Also the fact that the LAD becomes too thin to be successfully segmented well before it has reached the apex often plays a role.

Figure 6c shows the coronary territories computed without artificially completing the coronary artery segmentation. In this particular case, the divergence from the 17-segment model is rather minor and correspondence is only lost in the apical segment of the model, corresponding to the inner ring. Since no constraints are set, the divergence may be arbitrarily large. In fact, the territories may even

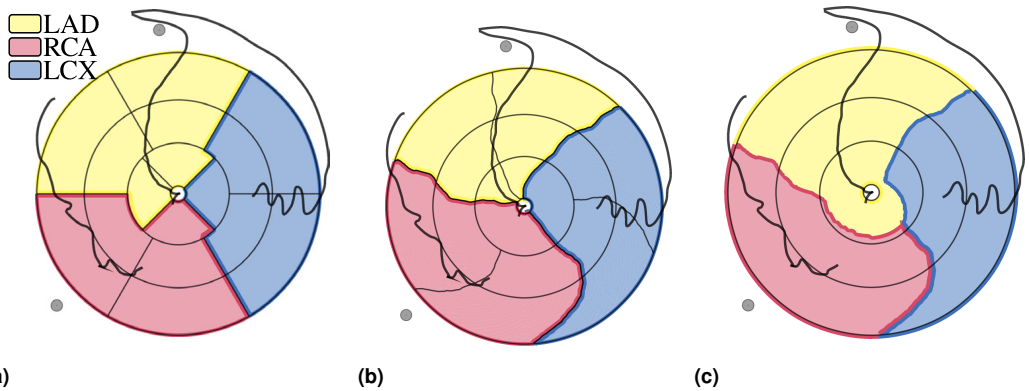


**Figure 6** A comparison of (a) the 17-segment model, (b) the 17-segment model adapted using the patient-specific coronary anatomy and (c) unconstrained coronary territories. The three coronary arteries are projected as black lines. All three bull's eye plots correspond to the same patient.

be disjoint, although this rarely occurs in practice. While this approach imposes less constraints on the coronary territories, it is also more sensitive to incomplete segmentations of the coronary arteries.

## 5 Medical Expert Evaluation

We have performed an informal evaluation of our approach by selecting five patients who underwent a whole-heart cardiac MRI scan and generating four bull's eye plots for each patient. The first bull's eye plot contained only a projection of the three primary coronary arteries. The second, third and fourth bull's eye plots also contained the original 17-segment model, an adapted 17-segment model and unconstrained coronary territories, respectively. Figure 6 gives the latter three bull's eye plots for patient 2 used in this experiment. For patient 4 an adapted 17-segment model could not be generated. This issue is further discussed in Section 6.

An experienced cardiologist first manually drew the coronary territories on the first bull's eye plot for each patient. The next task was to rate the correspondence between the projected coronary arteries and the coronary territories as produced by each of the three approaches on a scale from one (very bad) to five (very good). The results of this evaluation are listed in Table 1.

| Case | Method 1 | Method 2 | Method 3 |
|---|---|---|---|
| Patient 1 | 5 | 5 | 5 |
| Patient 2 | 4 | 4 | 4 |
| Patient 3 | 2 | 2 | 4/5 |
| Patient 4 | 1 | N/A | 4/5 |
| Patient 5 | 1 | 2 | 4/5 |

**Table 1** Results of our evaluation experiment. Method 1 corresponds to the original 17-segment model, method 2 corresponds to the adapted 17-segment model and method 3 corresponds to using unconstrained coronary territories. The scale ranges from one (very bad) to five (very good).

Finally our expert provided an overall rating for each approach of determining coronary artery territories. The manual approach was given a score of 4, both the original and our adapted 17-model were rated 3 and using unconstrained coronary territories was rated 4.

Our expert expressed that it was difficult to get a feeling for the concept of forcing the coronary territories to correspond to the 17-segment model. The continuous bull's eye plot projection we used also created some confusion. It was not clear whether strong variations within one ring, such as in the lower right part of Figure 6c, corresponded to epicardial and endocardial territories or whether the diagram should be interpreted as having infinitely many rings. Finally, a suggestion was made to restrict the segmentation of the LAD in the inferior wall, as current segmentations often led to an overestimation of the LAD territory. This is also the reason why we were unable to compute constrained coronary territories for patient 4.

In the manually drawn territories the inner ring was entirely allocated to the LAD in all patients except the first. Since this does not correspond to the original 17-segment model, this was only reflected by the unconstrained coronary territories. This is clearly visible in the scores given in Table 1 and is also the primary reason this method is preferred. In summary, our expert was positive about our work, especially the unconstrained coronary territories. Our evaluation indicates that this approach can compete with a manual approach.

## 5.1 Application to CT Data

We have also applied our technique to a whole heart CT scan. We applied the same segmentation techniques as for the MRI scans. Due to the better spatial resolution of CT, we were able to extract a more detailed coronary artery tree. Figure 7 shows the unconstrained coronary territories of this dataset. We use hue to encode to which primary coronary artery a territory belongs to and use lightness to distinguish territories from subbranches. This visualizes the hierarchy in the coronary artery tree. It also demonstrates that our approach is capable of generating a large number of territories. Due to the more fine-grained segmentation of the coronary artery tree, there is little difference when the end points of the coronary arteries are connected to the apex. For the same reason as before, forcing correspondence to the 17-segment model was not feasible for this patient.

## 5.2 Application to Viability Data

The primary advantage of patient-specific information on the coronary territories is that it allows to establish a more accurate relation between a functional deficit and the coronary arteries. This involves including other types of data, such as cine, late enhancement and perfusion data. Here we give an example of how our approach can be combined with viability information from a late enhancement scan. A late enhancement scan shows areas where a contrast agent has accumulated, typically indicating dead tissue called scar. We demonstrate that the patient-specific coronary territories can lead to a better understanding of which coronary arteries are related to areas of scar.

Figure 8 shows two bull's eye plots that each depict both the coronary territories and viability data. The darker areas in the bull's eye plots correspond to areas of scar. The top bull's eye plot shows the coronary territories as an adapted 17-segment model. In the bottom bull's eye plot, we adapted the volume data to fit the original 17-segment model using the inverse of function $f$ discussed in Section 4.1. We implemented this using on-the-fly resampling of the volume data. In other words, function $f^{-1}$ is evaluated for every pixel during the rendering of the bull's eye plot. In this case the scar on the top side of the bull's eye plot is stretched to fill the entire segment.

On the right of Figure 8 a three-dimensional view is shown to relate the scar to the three-dimensional coronary and cardiac anatomy. The coronary territories are projected on the epicardial surface, using the adapted 17-segment model approach. To establish a strong correspondence between the bull's eye plot and the three-dimensional view, we show a cursor on both views, indicated by the red arrows in Figure 8. To facilitate easy navigation, the viewpoint can be controlled by the position

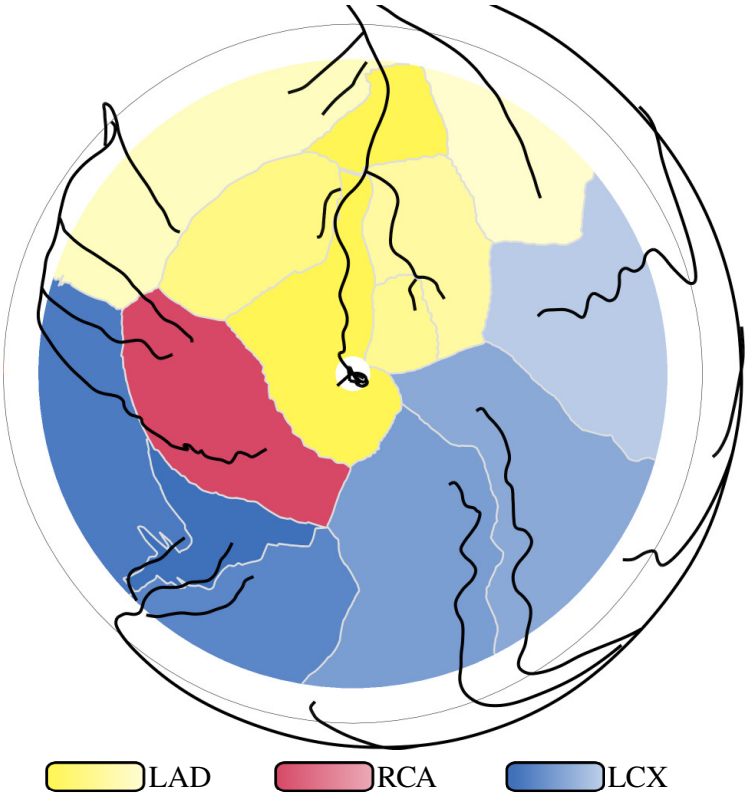


**Figure 7** Unconstrained coronary territories computed from a detailed coronary artery tree extracted from a CT scan. The hue of each territory encodes its primary coronary artery, while the lightness is used to distinguish territories from subbranches.

of the cursor. The user can then explore the three-dimensional view by moving the cursor on the bull's eye plot.

## 6 Discussion

For some patients, the coronary anatomy is too different from what the 17-segment model assumes. As was verified by Pereztol-Valdés *et al.* [10] and Ortiz-Pérez *et al.* [9], especially in the apical region there is a lot of variance among patients. Figure 9a shows the unconstrained coronary territories of one of our patients. The territory of the LAD is relatively large because the LAD covers both the anterior and inferior left ventricular walls in the apical area. Moreover, the part of the RCA that was visible in the whole heart MRI scan did not extend toward the apical region.

For this patient, our approach of adapting the 17-segment model fails since we cannot force a correspondence due to the dominant LAD. If an adapted 17-segment model is desired, the segmentation of the LAD could be restricted in the apical area. Analyzing the unconstrained coronary territories as shown in Figure 9a is in fact especially useful for patients with a coronary anatomy that considerably diverges from the average.

There are also patients that correspond very well to the 17-segment model. Figure 9b shows a comparison of an adapted 17-segment model and the standard 17-segment model in red and black lines, respectively. For this particular patient, the edges of the coronary territories map fairly well to what the 17-segment model predicts. It should be noted however that the model of each part of the myocardium being exclusively perfused by a single artery is especially inaccurate near these borders

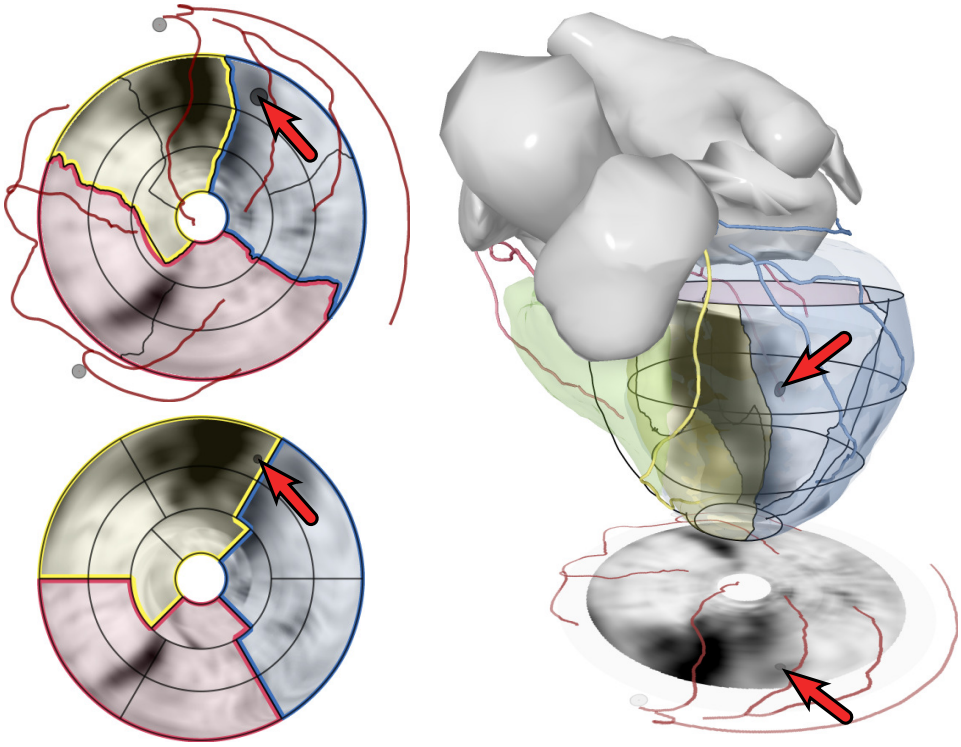

**Figure 8** Combined visualization of coronary territories and viability information. The darker areas in the bull's eye plots and the three-dimensional view correspond to areas of scar. A cursor (red arrows) shows corresponding points on both bull's eye plots and the three-dimensional view. The 17-segment model is shown in the three-dimensional view as a set of black lines around the epicardium.

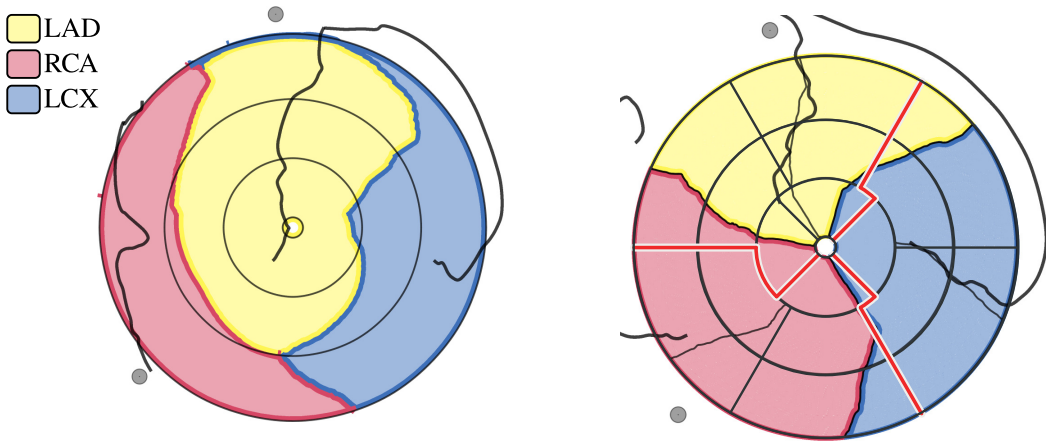


**Figure 9** Varying correspondence to the 17-segment model: (a) a case where adapting the model fails, (b) a case with relatively little difference to the model.

of the coronary territories. Another aspect that is visible in Figure 9b is that due to the circular nature of the bull's eye plot, differences near the apex result in smaller visual differences in the diagram.

We have not included segment number 17, corresponding to the apex, in our experiments. This segment forms a special case compared to the other 16 segments. It it is connected to all other territories and only has one border. A special approach is required to assign it to a coronary territory, since there is no clear mapping between this segment and the Voronoi diagram on the epicardial mesh. Thus when adapting the 17-segment model, it would only have to be decided to which coronary territory this segment should be assigned, but no edges need to be adjusted.

In our experiments we used meshes consisting of approximately $10^4$ quadrilaterals. The entire preprocessing phase, including the mesh computation, coronary artery projection, Voronoi diagram computation and computing the adapted 17-segment models typically takes less than one second on a modern workstation (Intel Xeon 3 Ghz, 2 GiB RAM, NVIDIA GeForce 8800 GTX).

## 7 Conclusion

We have introduced two approaches for establishing a relation between the patient-specific coronary anatomy and the myocardium. In the first approach we adapt the borders of the segments of the 17-segment model as defined by the American Heart Association. In the second approach we compute the coronary territories without taking any model into account. Both approaches are based on a Voronoi diagram computation of the coronary arteries projected onto a quadrilateral mesh of the epicardium.

Both approaches provide detailed insight in the patient-specific coronary anatomy. Adapting the 17-segment model forces a correspondence between the coronary territories and the 17-segment model by connecting the end points of the primary coronary artery branches to the apex. This approach forms a compromise between using a model-based approach and a segmentation-based approach. The second approach does not pose any constraints and thus allows for arbitrarily shaped coronary territories. It is therefore also more sensitive to incomplete segmentations of the coronary arteries. While the uniformity appearance of the 17-segment model is lost, the additional patient-specific information on the coronary territories allows for a better understanding on the relation between the coronary arteries and the myocardium.

We have presented an application of using patient-specific coronary territories with visualizing viability information from a late enhancement scan. Instead of altering the 17-segment model to correspond to the coronary anatomy, we show that it is also possible to fit the underlying volume data to the original 17-segment model. This approach creates uniformly looking bull's eye plots, regardless of the coronary anatomy of the patient.

Feedback obtained through an evaluation experiment with a cardiologist gave a clear signal that our work has clinical relevance. Results indicated that there is a preference towards using unconstrained coronary territories. The latter method produced territories that best matched those indicated manually by our cardiologist and are considered to have a greater correspondence than those that the original 17-segment model suggest.

## Acknowledgements

This work was performed in the scope of the COMRADE project funded by Philips Healthcare, Best, The Netherlands. The datasets were provided by Hyogo BHC at Himeji and the Tokyo Metro Police Hospital.

## References


1 American Society of Nuclear Cardiology. Imaging guidelines for nuclear cardiology procedures. *J Nuclear Cardiology*, 6:G47–G48, 1999.

2 P. Beliveau, R.M. Setser, F. Cheriet, R.D. White, and T. O'Donnell. Computation of coronary perfusion territories from CT angiography. *Computers in Cardiology*, 34:753–756, 2007.

3 Pascale Beliveau, Randolph Setser, Farida Cheriet, and Thomas O'Donnell. Patient-specific coronary territory maps. *Proc. SPIE*, 6511:65111J, 2007.

4 Manuel D. Cerqueira, Neil J. Weissman, Vasken Dilsizian, Alice K. Jacobs, Sanjiv Kaul, Warren K. Laskey, Dudley J. Pennell, John A. Rumberger, Thomas Ryan, and Mario S. Verani. Standardized myocardial segmentation and nomenclature for tomographic imaging of the heart. *Circulation*, 105:539–542, 2002.

5 Olivier Ecabert, Jochen Peters, and Jörgen Weese. Modeling shape variability for full heart segmentation in cardiac computed-tomography images. In *Proc. SPIE*, volume 6144, pages 1199–1210, 2006.

6 Rufold Karch, Friederike Neumann, Martin Neumann, Paul Szawlowski, and Wolfgang Schreiner. Voronoi polyhedra analysis of optimized arterial tree models. *Annals of Biomedical Engineering*, 31:548–563, 2003.

7 Cristian Lorenz, Steffen Renisch, Thorsten Schlathoelter, and Thomas Buelow. Simultaneous segmentation and tree reconstruction of the coronary arteries in MSCT images. In *Proc. SPIE*, volume 5031, pages 167–177, 2003.

8 S. Oeltze, A. Kuß, F. Grothues, A. Hennemuth, and B. Preim. Integrated visualization of morphologic and perfusion data for the analysis of coronary artery disease. In *Proc. EuroVis*, pages 131–138, 2006.

9 José T. Ortiz-Pérez, José Rodríguez, Sheridan N. Meyers, Daniel C. Lee, Charles Davidson, and Edwin Wu. Correspondence between the 17-segment model and coronary arterial anatomy using contrast-enhanced cardiac magnetic resonance imaging. *JACC: Cardiovascular Imaging*, 1(3):282–293, 2008.

10 Osvaldo Pereztol-Valdes, Jaume Candell-Riera, Cesar Santana-Boado, Juan Angel, Santiago Aguade-Bruix, Joan Castell-Conesa, Ernest V. Garcia, and Jordi Soler-Soler. Correspondence between left ventricular 17 myocardial segments and coronary arteries. *European Heart Journal*, 26:2637–2643, 2005.

11 O. M. Weber, A. J. Martin, and C. B. Higgins. Whole-Heart Steady-State Free Precession Coronary Artery Magnetic Resonance Angiography. *Magnetic Resonance in Medicine*, 50(6):1223–8, 2003.